Evolution of beam-foil-excited Rydberg states on femtosecond time scales

E. P. Kanter, R. W. Dunford, D. S. Gemmell, M. Jung, T. LeBrun,* K. E. Rehm, and L. Young
Argonne National Laboratory, Argonne, Illinois 60439
(Received 20 July 1999; published 9 March 2000)

Traditional beam-foil methods for measuring lifetimes of low-lying atomic levels are generally impractical beyond $Z\sim35$ because of the correspondingly shorter flight times when lifetimes become less than a few tens of picoseconds. We recently reported the results of an experiment using a novel two-foil method to measure the 9.5-psec lifetime of the $2\,^3P_2$ level in heliumlike krypton. We describe here the results of an extension of that work in which we measured the time evolution of the $N\geqslant2$ excited state population between the foils by observing the dependence upon foil separation of the charge-state distributions emerging from the second foil. The results are consistent with the well-known power-law dependence of Rydberg-fed atomic transitions observed in beam-foil studies, but probe a much shorter time scale than has hitherto been accessible.

PACS number(s): 34.50.Fa, 39.90.+d

I. INTRODUCTION

The penetration of swift heavy ions through solids is a subject that continues to interest investigators despite more than 50 years of intense study. In addition to the intrinsic interest in the collisional processes involved, a large part of the continuing fascination with this problem stems from several important applications, such as the design of heavy-ion accelerators and beam-foil spectroscopy experiments, which require knowledge of the charge- and excited-state distributions of fast ion beams exiting from stripping foils.

Despite this interest, there is as yet no comprehensive method to compute reliably such distributions from first principles. The crux of the problem lies in the very high electronic densities of solid targets, which means that collisional mean free paths are generally short in comparison to the field-free excited-state lifetimes. Consequently, the exciting collisions cannot be treated independently. Further, one must deal with complex multiply-excited systems in the environment of the solid where there are strong electric fields present with large dc and fluctuating components. The resulting n,l and charge-state distributions are markedly different from those resulting from ion-atom collisions in gas targets. In particular, foil-excited ions emerge more highly excited and in higher charge states than do gas-excited ions of the same velocity for media with similar atomic numbers [1].

The importance of understanding excited-state populations was recognized in the earliest days of beam-foil spectroscopy [2] when it was first observed that cascades from long-lived, highly-excited states can cause significant repopulation of relatively short-lived states [3]. This complicated the extraction of lifetimes of lower-lying excited states. It has been observed that such cascades always lead to a long-lived component to any low-lying prompt transition, which exhibits a characteristic power-law time dependence [4].

We report here the results of an experiment that is sensitive to such cascade repopulation at extremely short times. We have previously demonstrated that by exploiting a precision two-foil target arrangement, we could measure ultrashort atomic lifetimes (i.e., 0.1–10 ps) with foil-excited beams [5]. The foils were parallel to each other and perpendicular to the beam velocity. The method is somewhat analogous to the recoil distance method used in nuclear spectroscopy [6] in that the second ''probe'' foil is used to sample the excited-state population that survives the transit time following the exit from the first ''exciter'' foil. In the earlier experiment we observed x-rays emitted downstream of the second foil and determined the lifetime of the $2\,^3P_2$ level in He-like Kr to be 9.5(9) ps.

In the present work, we have extended those measurements to include the charge-state distributions of emergent ions downstream of the second foil. By varying the distance between foils with a resolution of 0.3 μm (corresponding to a time resolution of 7 fs), we are able to observe the preferential quenching of excited electronic states in the second foil. We show that such measurements can serve as a sensitive probe of the cascade repopulation process at extremely short times (a few fs after the ions exit the first foil) and thus provide an important test of the n,l distributions of foil-excited Rydberg states.

II. EXPERIMENTAL PROCEDURE

A beam of $^{84}Kr^{19+}$ ions was obtained from the Argonne Tandem Linac Accelerator System (ATLAS) at an energy of 700 MeV. Upon exiting ATLAS, these ions were further stripped in a 200-μg/cm^2 carbon foil. About 35% of the beam emerged from the stripper foil as heliumlike Kr^{34+}, which was then selected by a magnet and directed toward the experimental chamber. The beam was collimated by a 2.5 $\times$2.5 mm^2 set of slits and then impinged upon the target assembly (see Fig. 1). Two thin self-supporting carbon targets could be mounted in this assembly and moved relative to each other with a precision of $\sim$1/3 μm.

Ions emerging from the second foil within $\pm4°$ of the beam direction were magnetically analyzed by an Enge split-pole spectrograph and detected by a position-sensitive parallel-plate avalanche detector in the focal plane [7]. The active area of the counter permitted the detection of all emerging ions with charge states in the range from 29+ to

*Present address: National Institute of Standards and Technology, Gaithersburg, MD 20899.

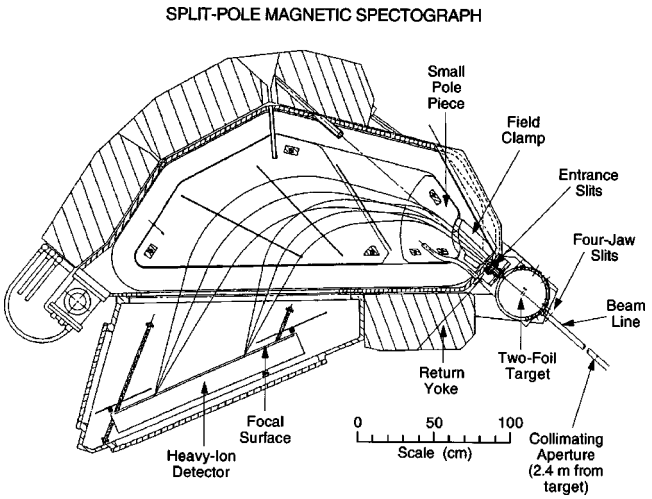

FIG. 1. Schematic view of the experimental setup used.

35+ with a single magnetic field setting. The beam intensity was reduced by a filter mesh at the ion source before acceleration. At all times the overall count rate on the detector was kept below 5 kHz.

Emergent charge-state distributions were measured as a function of foil separation by moving the translation stage and counting for a fixed number of ions striking the detector. This value ($\sim 10^5$–10^6) was chosen so that, in most cases, the weakest charge-state fraction observed was determined to a relative accuracy $\sim 1\%$.

III. RESULTS

In order to optimize the target thicknesses, and for comparison to the two-foil results, some preliminary measurements were carried out with single foil targets. Some of these final charge-state distributions are shown in Fig. 2 for 700-MeV Kr^{34+} ions traversing carbon foils of various thicknesses (x). The mean charges determined from each of the measured single foil charge-state distributions are shown in

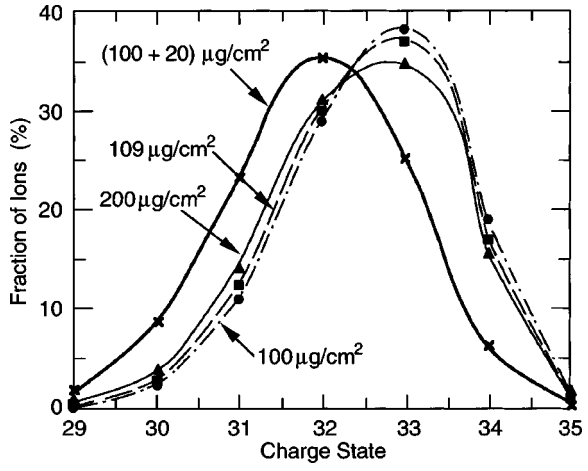

FIG. 2. Charge-state distributions for 700-MeV Kr^{34+} ions emerging from carbon foils of 100, 109, and 200 $\mu g/cm^2$ thickness. Also shown is the distribution measured after penetrating two foils of 100 and 20 $\mu g/cm^2$ separated by 16 mm.

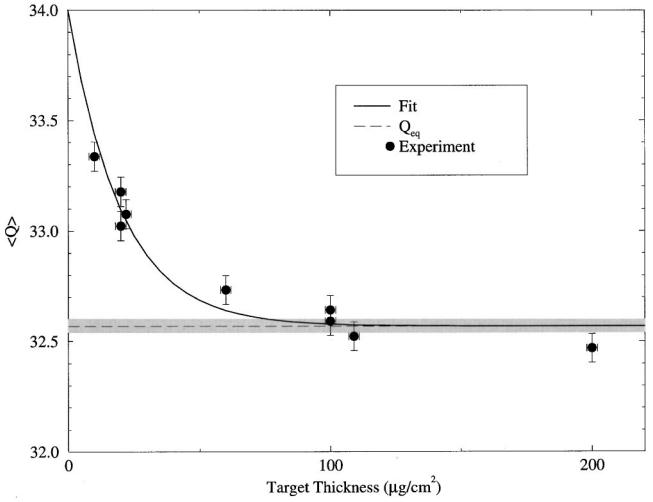

FIG. 3. Mean charges determined from the charge-state distributions for 700-MeV Kr^{34+} ions emerging from carbon foils of varying thicknesses between 10–200 $\mu g/cm^2$. The solid line shows the fit to the data described in the text. The dashed line represents the equilibrium charge extracted from that fit.

Fig. 3. These data were fitted to

$$\overline{q} = q_\infty + (q_0 - q_\infty)\exp\left(\frac{-x}{\lambda}\right), \tag{1}$$

where q_∞ is the equilibrium mean charge, q_0 the incident charge (34+), and λ the mean free path for charge-changing collisions as determined by the total charge-changing cross section and the target electron density n:

$$\lambda = \frac{1}{n\sigma_{tot}}. \tag{2}$$

The result of this fit is also shown in Fig. 3. From the fit, we find $\lambda = 20(2)$ $\mu g/cm^2$ and $q_\infty = 32.57(3)$. This is in good agreement with the value of 32.4 obtained from a semiempirical formula [8]. Using Eq. (2) we find $\sigma_{tot} = 1.0(1) \times 10^{-18}$ cm^2.

It is apparent from the data of Figs. 2–3 that the charge-state distributions are essentially equilibrated for foil thicknesses $\geqslant 100$ $\mu g/cm^2$. In Fig. 2, we also show the charge-state distribution measured after the ions emerge from a two-foil target composed of a 100-$\mu g/cm^2$ carbon foil followed by a 20-$\mu g/cm^2$ carbon foil. The interfoil distance was relatively large (~ 16 mm) and corresponds to a flight time of ~ 0.4 nsec. Based on the previous findings, the first foil is sufficiently thick (100 $\mu g/cm^2$) to produce an equilibrium distribution, yet the addition of the second foil upsets this equilibrium. The presence of the interfoil gap has a dramatic effect in shifting the distribution to *lower* charge states. As we will describe below, this is a consequence of the excited state population produced in the first foil relaxing during the relatively large transit time between foils. This difference between stripping in a single foil and the separated foils is reminiscent of the difference between gaseous and solid strippers in the Bohr-Lindhard model [9] of ion penetration. In this model, the high frequency of exciting collisions in a

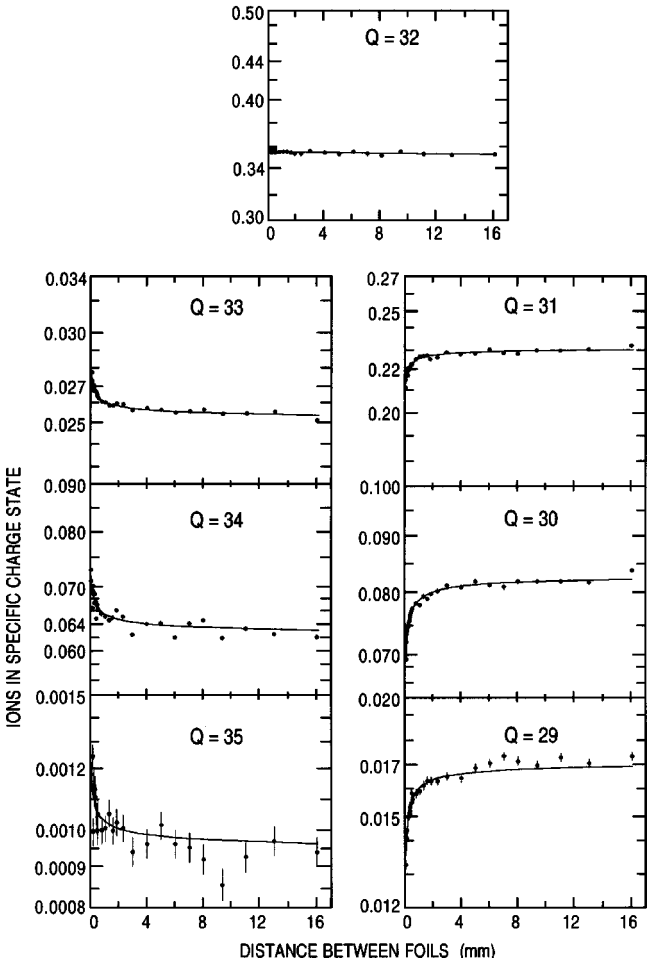

FIG. 4. The fraction of each final charge state for 700-MeV Kr^{34+} ions emerging from a pair of carbon foils (100 $\mu g/cm^2$ followed by 20 $\mu g/cm^2$ thickness). The solid line represents the fit described in the text.

solid target does not permit as much time for radiative decay as in a gas target, and thus leads to a higher degree of both excitation and ionization by successive collisions in the solid. In our experiment, the interfoil gap plays a role similar to a very diffuse gas by extending the mean free path (in this case macroscopically) and thus permitting sufficient time for more of the excited-state population to radiate before reentering the solid. The second foil is of subequilibrium thickness (20 $\mu g/cm^2$) and thus the charge-state distribution emerging from it is still somewhat dependent on the *initial* excitation state. In particular, electron loss cross sections depend explicitly on binding energies and hence are sensitive to the initial excitation state of the projectile. By contrast, capture cross sections are determined by the wave function overlap of the captured target electron with the projectile *final* state and thus are generally insensitive to projectile excitation. Hence, following the interfoil relaxation, the average electron-loss cross sections in the thin second foil are generally smaller for the more tightly bound relaxed ions, leading to lower charge states emerging from that foil.

The complete set of two-foil data is shown in Fig. 4, which presents the fractions in each final charge state as a function of the interfoil distance from ''0'' (our minimum distance was $<1\mu$) to 16 mm. These data were taken with 700-MeV Kr^{34+} ions incident on a 100-$\mu g/cm^2$ carbon foil followed by a second carbon foil of 20 $\mu g/cm^2$. At the largest separation, the most probable exit charge state was 32+ (see Fig. 2). Emergent ions in charge states lower than this value (29–31+) generally increase in yield with increasing foil separation, while the higher charge states (33–35+) all show a decrease. The 32+ fraction appears to be essentially independent of foil separation. Thus, as the foil separation *decreases*, the average charge state *increases*.

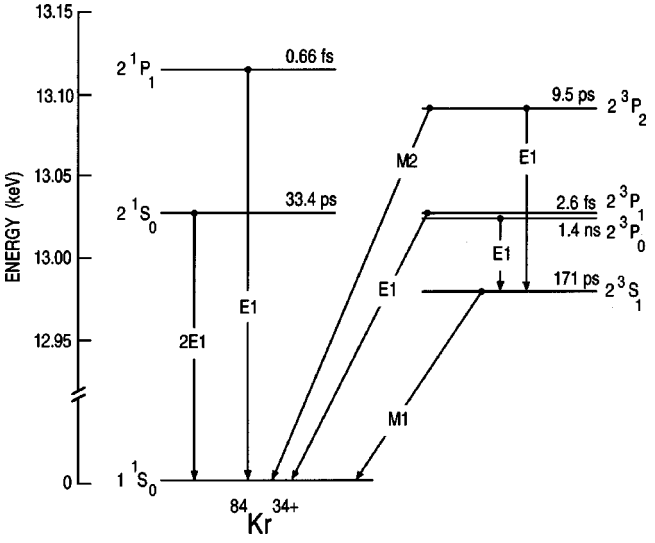

FIG. 5. Low-lying energy levels of He-like krypton showing decay modes and lifetimes.

IV. DISCUSSION

In our earlier experiment, we observed the dependence of the K x-ray emission yield downstream of the two-foil target on the interfoil distance under conditions identical to this measurement [5]. We found that yield to depend strongly on the surviving $n=2$ population entering the second foil that on this timescale was dominated by the 9.5-ps $2\,^3P_2$ and 171-ps $2\,^3S_1$ levels in He-like Kr. In Fig. 5 we show a diagram of the $n=1$ and $n=2$ levels in He-like krypton giving the energies and lifetimes. The 2^3P_2 level decays to the ground state by $M2$ emission and to the $2\,^3S_1$ level via $E1$ emission. For krypton, theory predicts that nearly 90% of the $2\,^3P_2$ states decay via the $M2$ branch. Since all other levels are either much shorter or much longer lived, the $2\,^3P_2$ and $2\,^3S_1$ levels dominated and produced a two-exponential decay curve.

The present data, measuring charge-state distributions and probing a much broader time scale, exhibit a more complicated behavior. In the first instance, all (except 32+) final charge-state populations depend on the interfoil gap. Second, we find that behavior to be governed by a power-law dependence on the foil distance rather than a few exponentials. For example, for the 35+ fraction, the fitted amplitude of an exponential component is $(1\pm140)\times10^{-6}$ while the amplitude of a power-law component is $(130\pm56)\times10^{-6}$ with a

normalized χ^2 of 1.3 (allowing the exponential lifetime and power to vary in a four-parameter fit). Similar results were found for the other charge-state populations. Such power-law decay curves are common in beam-foil spectroscopy when the observed level is being fed by longer-lived cascades from higher-lying Rydberg states [10]. On the time scale sampled in this experiment, Rydberg states as high as $n=100$ could contribute to the excited-state population between the foils at the largest separation. Hence, in view of the integral nature of charge-state distributions in averaging over excited-state populations, it is not unreasonable to expect such cascades to dominate the interfoil decay.

As a result of these considerations, we propose a simple two-component model to describe these data. Consider those ions exiting the first foil in the ground state (regardless of charge state) to be ''relaxed'' and the remainder ''excited.'' The relaxed ions traverse the interfoil distance and then penetrate the second thinner, subequilibrium foil. These ions then emerge from the second foil in a distribution of charge states $f(q)$, which we define as ''normal.'' The excited-state population evolves during transit of the interfoil gap and either decays, enhancing the ''relaxed'' population, or enters the second foil with residual excitation. In general, because of the reduced electron binding energies in excited states, electron-loss cross sections are increased. Because of the subequilibrium thickness of the second foil, these modified cross sections imply a modified charge-state distribution $g(q)$, which will be shifted to somewhat higher mean charges for the ''excited'' fraction. Assuming the excited-state population decays through cascades with a time dependence given by $1/t^m$, the surviving population entering the second foil after an interfoil flight time t will be given by

$$P_{n>1}(t)=\sum_{n>1} P_n(0)-\int_0^t I_{n=2\rightarrow 1}(t')dt' \tag{3}$$

$$=C_0+C_1 t^{-m+1}, \tag{4}$$

where $I_{n=2\rightarrow 1}(t)$ is the cascade-fed intensity of Lyman-α radiation and the level index $n=1$ corresponds to ground-state ions and $n>1$ to all excited states. The power-law dependence of $I_{n=2\rightarrow 1}(t)$ has been shown to hold on quite general grounds, however the power m can depend quite sensitively on the initial n,l distribution [11] and hence we treat it as a free parameter to be determined by fitting the data.

Assuming that $P_{n>1}(t)\rightarrow 0$ as $t\rightarrow\infty$, implies that

$$P_{n>1}(t)=a_0 t^{-m+1}. \tag{5}$$

Combining $f(q)$ and $g(q)$ with this result, we expect the measured charge-state distribution to evolve with interfoil dwell time as

$$F(q,t)=P_{n>1}(t)g(q)+[1-P_{n>1}(t)]f(q). \tag{6}$$

We have fitted all the data in Fig. 4 with Eq. (6) and the results are shown as the solid line in that figure. The distribution $f(q)$ was taken to be the relaxed distribution measured at the largest separation. The fit determines nine free parameters [a_0, m, and the $g(q)$ distribution]. We find $a_0=0.0893(5)$ and $m=1.443(6)$. Care should be exercised in the interpretation of m since it represents a global average behavior of the excited-state populations in all charge states, yet the value extracted here is in generally good agreement with the values obtained in observations of cascade-fed Lyman-α radiation in hydrogenlike heavy ions [12–14].

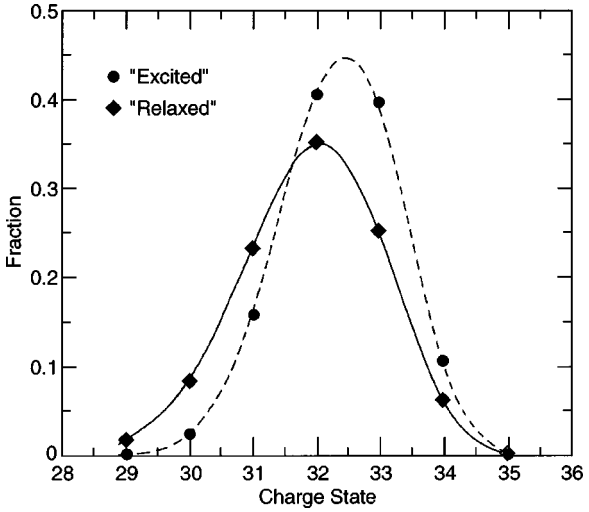

FIG. 6. Charge-state distributions for 700-MeV Kr^{34+} ions emerging from a pair of carbon foils (100 μg/cm^2 followed by 20 μg/cm^2 thickness). The diamonds show the distribution $f(q)$ corresponding to ions entering the second foil in their ground states as measured at the largest foil separation. The filled circles represent the distribution $g(q)$ of excited ions extracted from the fit procedure described in the text. The lines are drawn to guide the eye.

The charge-state distribution produced in the second foil by the excited-state population $g(q)$ is shown in Fig. 6 together with the ''normal'' distribution $f(q)$. As anticipated, $g(q)$ is shifted up by roughly half a unit of charge compared to $f(q)$ demonstrating the enhanced loss cross section expected for the excited-state component of the beam.

As noted earlier, this effect is naturally described in the Bohr-Lindhard model. Some time ago, Betz and Grodzins pointed out the deficiency of that model with regard to the apparent similarity of the stopping powers of gases and solids [15]. They described a competing model where post-foil Auger processes account for the higher charge states emerging from foils. The present data, however, cannot be described by such a picture because post-foil Auger decays would lead to an *increasing* mean charge with increasing foil separation in contrast to our observations.

V. SUMMARY

We have demonstrated a method to probe the decay of very-highly-excited states in fast heavy-ion beams at time scales down to ~20 fsec and have shown the decaying population to be described by a power law over a broad time scale. Using a two-foil target, we observed a marked shift in ''equilibrium'' charge-state distributions as a function of the interfoil distance. With the aid of a simple two-component model (''relaxed'' and ''excited'' ions), we were able to account for these observations and have extracted both the de-

cay profile and the charge-state distribution produced by the excited ions in the second foil. These data demonstrate the validity of the Bohr-Lindhard model in this instance. Further refinements in these measurements, such as studies of the dependence on the thickness of the second foil, should permit the extraction of charge-changing cross sections for the excited ions as well.

ACKNOWLEDGMENTS

We thank J. Greene for preparation of the target samples and C. A. Kurtz and B. J. Zabransky for excellent technical support. This work was supported by the U.S. Department of Energy, Office of Basic Energy Sciences, Division of Chemical Sciences under Contract No. W-31-109-Eng-38.

[1] N. O. Lassen, Phys. Rev. **79**, 1016 (1950).
[2] W. S. Bickel and A. S. Goodman, Phys. Rev. **148**, 1 (1966).
[3] P. Richard, Phys. Lett. **45A**, 13 (1973).
[4] R. M. Schectman, Phys. Rev. A **12**, 1717 (1975).
[5] S. Cheng *et al.*, Phys. Rev. A **50**, 2197 (1994).
[6] T. K. Alexander, K. W. Allen, and D. C. Healey, Phys. Lett. **20**, 402 (1966).
[7] K. E. Rehm and F. L. H. Wolfs, Nucl. Instrum. Methods Phys. Res. A **273**, 262 (1988).
[8] H.-D. Betz, Rev. Mod. Phys. **44**, 465 (1972).
[9] N. Bohr and J. Lindhard, K. Dan. Vidensk. Selsk. Mat. Fys. Medd. **28**(7), 1 (1954).
[10] L. J. Curtis, Am. J. Phys. **36**, 1123 (1968).
[11] R. W. Hasse, H.-D. Betz, and F. Bell, J. Phys. B **12**, L711 (1979).
[12] A. P. Georgiadis *et al.*, Z. Phys. A **300**, 277 (1981).
[13] C. Can, R. J. Maurer, B. Bandon, and R. L. Watson, Phys. Rev. A **35**, 3244 (1987).
[14] R. W. Dunford *et al.*, Phys. Rev. A **48**, 2729 (1993).
[15] H. D. Betz and L. Grodzins, Phys. Rev. Lett. **25**, 211 (1970).